Crack propagation in plates and shells subjected to bending and direct loading

J. G. WILLIAMS and R. D. EWING
Mechanical Engineering Department, Imperial College, London

Summary
Tests on plates subjected to bending are described and it is found that the theoretical analysis must be modified to account for the edges of the crack touching on the compression side. Circular plates subjected to lateral pressure which fail in bending exhibit the same behaviour while for those in which large bulging occurs a tensile failure criterion is obeyed. Cylinders subjected to internal pressure with both axial and circumferential cracks conform to the theoretical expectations.

Introduction

The work described here arose from a need to apply the concepts of fracture mechanics to the design of engineering structures. Systems subjected to tensile stresses are described by the basic infinite plate form:

$$K = \sigma\sqrt{\pi a} \tag{1}$$

where σ = applied gross stress
a = crack length
K = stress intensity factor which has a critical value K_{Ic} at fracture.

This form has wide applicability for small cracks and is of considerable importance in design. Finite width and geometrical effects can be incorporated and many standard solutions are available [1, 2] for simple geometries. Some cases of considerable practical importance have not been widely studied and among these is the design of plate and shell structures.

The basis of the problem is that a bending stress system is applied to plate or shell and the stress system at the crack tip, instead of being constant, varies through the thickness of the sheet. Plate problems are an obvious example of this and the first part of this work will deal with rectangular plates subjected to bending moments and circular plates subjected to lateral pressure. Both are systems with almost entirely bending stresses and they provide a useful means of studying the effects of such stress systems.

Symmetrical shell structures subjected to internal pressure give rise to direct stresses only but the presence of cracks introduces asymmetry into the system and local bending actions are introduced. In this work cylinders with both axial and circumferential cracks will be examined. Thus a range of geometries and loading conditions is considered in an attempt to understand the effects of lateral bending.

All the tests described here were performed on polymethylmethacrylate (PMMA) as it is a convenient material and obeys the laws of fracture mechanics [3]. The cracks were formed by forcing a razor blade into a slot with a prescribed load and time under load by means of a hardness machine. Natural cracks formed in front of the blade and are necessary to give consistent results.

Plates subjected to bending

The system to be examined is shown in Fig. 1 and has been considered theoretically [4]. The analysis is in terms of the maximum bending stress σ_B and is given by:

$$\sigma_B = \frac{6M}{t^2} \tag{2}$$

where M = the applied bending moment per unit length
and t = the plate thickness.

It is concluded that an equation of the same form as (1) results but that the value of K is changed and given by:

$$K_B = \frac{3+\nu}{1+\nu} \cdot K. \tag{3}$$

There is some experimental evidence to support this result [5]. In these tests plates of PMMA were centrally notched and subjected to pure bending and the resulting graphs of log σ_B versus log a were approximate straight lines with slopes of about 0·5. The K values approximated to those predicted by equation (3).

Preliminary tension tests

A series of single edge notch tension tests were performed on the material to be used. The specimens were 2 in wide and 6 in long and the cracks were up to 0·3 in long. The tests were performed in an Instron testing machine and the specimens were loaded continuously to failure with loading times of approximately 15 secs. No account of slow crack growth is made in the analysis as for design purposes the original crack length is considered the important parameter. The results are plotted as σ versus $1/\sqrt{a}$ and the graph is shown in Fig. 2 indicating a good straight line and a K_{Ic} value of 1,020 lbf/in$^{3/2}$. No finite width corrections were made but these would only affect the lower values slightly and for comparison purposes the results are preferable in the form given here.

Bending tests

The apparatus used is shown in Fig. 3 and consists of two arms attached to the specimens as shown. The load was applied by the testing machine via pin joints and was increased continuously until the specimen broke with a loading time of 3-10 min. The bending moment at failure was calculated as:

$$M = PX$$

and the precise value of X was determined from a calibration curve. Values of X up to 3 in were used and the results were found to be independent of the value chosen. The system does not produce pure bending as there is tensile stress given by:

$$\frac{\sigma_T}{\sigma_B} = \frac{t}{6X}.$$

As the largest t used was 0·25 in and the smallest X was about 1 in, the ratio never exceeded 1/24. Thus the tensile stress was ignored and it was assumed that the stress was entirely bending. Tests were performed on $\frac{1}{8}$ in and $\frac{1}{4}$ in specimens with widths of 2, 3 and 4 in and the results are shown in Fig. 4 plotted as σ_B versus $1/\sqrt{a}$.

Comparison with the simple tension line taken from Fig. 2 and the line given by equation (3) shows that neither is a good representation of the points. There is considerable scatter (±10%) which is probably due to the fracture starting at the surface and thus being more sensitive to imperfections.

The slow growth was easily observed because of the rough surface of these regions. The amount varied with initial crack length and without exception had an elliptical form as shown in Fig. 5. Measurements were made using a projection microscope and graphs of x^2 versus y^2 (the two coordinates) gave straight lines, Fig. 6, indicating the elliptical form:

$$\frac{x^2}{b^2} + \frac{y^2}{c^2} = 1.$$

This is in contrast to [5] which mentions triangular slow growth areas.

Pressure tests on circular plates

The apparatus used is shown diagrammatically in Fig. 7. The specimen is clamped in position and the water level is adjusted with valve A closed by filling the pressure vessel. Valves B and C are then closed and A opened to apply pressure to the gas-water interface. Valve A is then closed and valve B opened slowly to apply the water pressure to the specimen.

The pressure is measured using a pressure transducer and recorded on a time based recorder. A trace of pressure versus time is thus obtained and the failure pressure determined. The loading time was kept approximately constant at 15 sec by controlling the rate of opening of valve *B*.

Specimens were tested with diameters of 6, 8 and 9 in and thicknesses of nominally ⅛ and ¼ in. Central slots of up to 1 in were machined in the discs and the ends formed in the usual way using a razor blade. Leakage through the slot was prevented using a light metal strip over the slot and a seal of plasticene.

As the crack lengths were small the bending stress over the crack was taken as the hoop bending stress at the centre of a flat plate and calculated from elasticity as:

$$\sigma_B = 0{\cdot}506\,\frac{p.R^2}{t^2} \tag{4}$$

for $\nu = 0{\cdot}35$.

In many tests there was a large bulging effect and in these cases equation (4) is obviously incorrect as the stress system is largely tensile. The criteria used to decide it (4) was valid was to calculate the central deflection δ using the measured failure pressure and if $\delta/t < 1$ then (4) was used. If $\delta/t > 1$ then the tensile stress was calculated using an approximate formulae given in [6]:

$$\sigma = 0{\cdot}423\left[\frac{Ep^2R^2}{t^2}\right]^{1/3} \tag{5}$$

using a vaule of E of $4{\cdot}5\times10^5$ lbf/in². The results are shown in Fig. 8 as the stress versus $1/\sqrt{a}$ as before.

Those plates which failed under bending ($\delta/t<1$) follow the same pattern as the previous bending results. The plates which had large bulging give much higher values of bending stress if this is calculated and with a large degree of scatter. When equation (5) is used the results show much less scatter, although it is still appreciable, as the criteria $\delta/t>1$ is an approximation. However, there is clear evidence that the behaviour is tensile in nature and follows the usual K laws.

In all the bending tests performed the geometric factors of size (W and R) and thickness (t) are shown to be accounted for in the calculations used for these small crack cases.

Cylinders under internal pressure

Early attempts at a theoretical analysis of this system [7] used the concept of treating the sides of the crack as an elastically supported beam and it was concluded that there was a dependence on the parameter a^2/Rt. A com-

plete analysis is now available which considers the details of the stress distribution including the interaction of tension and bending [8, 9, 10] and for the case of internal pressure only is given in the form:

$$\frac{k^2}{\pi\sigma^2 a} = 1 + C\,.\,\lambda^2 \tag{6}$$

where C = a constant depending on the crack configuration

and $\lambda^2 = \sqrt{12(1-\nu^2)}\,.\,\dfrac{a^2}{Rt}$.

The form is theoretically valid for $\lambda^2<1$ as other terms in λ^4 ln λ are ignored. For $\nu = 0{\cdot}35$ this becomes:

$$\lambda^2 = 3{\cdot}42\,.\,\frac{a^2}{Rt}.$$

For an axial crack $C = 0{\cdot}49$ and equation (6) becomes:

$$\frac{K^2}{\pi\sigma^2 a} = 1 + 1{\cdot}67\,.\,\frac{a^2}{Rt} \tag{7}$$

(σ = hoop stress)

and for a circumferential crack $C = 0{\cdot}098$ and

$$\frac{K^2}{\pi\sigma^2 a} = 1 + 0{\cdot}34\,.\,\frac{a^2}{Rt}. \tag{8}$$

(σ = axial stress)

Equation (7) has been investigated experimentally by several authors [e.g. 11] and found to be a good representation of results and is accurate for values for λ up to 3·4 and reasonably so for values up to 8·2. This gives the following range a^2/Rt:

Accurate up to 3·4
Reasonably accurate up to 20

which is due to the small effect of additional terms in this range.

The specimens used were ⅛ and ¼ in thickness and with diameters of 2, 3 and 4 in. Discs of the same material were fitted into the ends of the cylinders and fixed with a cementing compound. The notches were made in the usual way by machining slots and forming the ends with a razor blade. The same pressure testing equipment was used with a different attachment on the clamp. The tests were performed by increasing the pressure continuously to give a loading time of about 15 sec and for axial cracks they are shown in Fig. 9 as $\sigma\sqrt{\pi a}$, where σ is the hoop stress, plotted against a^2/Rt.

The most notable feature of the crack surface was the complete absence of slow growth. In all the bending tests the slow growth could be seen forming but in the tube tests catastrophic failure was immediate. The results show a single line when plotted against a^2/Rt and they tend to an initial value considerably above 1020 lbf/in$^{3/2}$. [3] suggests a value of 1,650 lbf/in$^{3/2}$ for no slow growth and this value is plotted in Fig. 9 with equation (7). There is good agreement up to about $(a^2/Rt) = 3$ but above this the theory would appear to be consistently below the experimental results.

Circumferential cracks presented special problems in that the stress levels at fracture are considerably higher and for the system used here failure occurred at the ends of the specimens if short cracks were used. Thus the value of a^2/Rt was limited to a minimum value of 4. The results are shown in Fig. 10 together with equation (8) and close agreement is apparent. In this case the theory appears to be much closer to the experiment at high a^2/Rt than for the axial cracks.

Discussion

The nature of fracture behaviour in PMMA as described in [3] will be repeated in outline here as a basis for this discussion. Difficulties in interpretation arise because K_{Ic} is a function of crack speed and it can be shown that if a crack starts slowly then the K_{Ic} value calculated on the basis of initial crack length will be in the range 800-1000 lbf/in$^{3/2}$ depending somewhat on the loading time and hence crack speed. Variations of this sort take place over some six decades of crack speed and thus no appreciable variation in K_{Ic} would be expected over the range in these tests (about 15 sec loading time in all but the bending tests which were 3-10 min). If, however, K_{Ic} is calculated when rapid fracture starts, taking the crack length plus the slow growth, then a K_{Ic} of about 1,600 lbf/in$^{3/2}$ results.

The simple tension results show how precisely PMMA obeys the laws of fracture mechanics and gives a basic value of the slow growth K_{Ic} for these conditions (1,020 lbf/in$^{3/2}$). The bending results were obtained at somewhat lower rates but this should not affect them greatly. Clearly they do not conform to the theoretical prediction of :

$$K_B = \frac{3+\nu}{1+\nu} \cdot K_T$$

and the most probable explanation is that mentioned in [12] in that when the specimen bends the lower edges of the crack touch and give a direct stress system along the crack surface. This violates the conditions of the analysis and poor agreement results. The effect would be expected to be less for long cracks where greater flexibility could dissipate the effect and this is borne out by the points tending to the line at low values of $1/\sqrt{a}$ in$^{-1/2}$.

A possible explanation of the behaviour is that there is an effective length, say $\bar{a}$, over which a nett tensile stress $\bar{\sigma}$ is developed. This force is distributed over the crack length and thus by equilibrium we have:

$$\sigma_T \cdot a = \bar{\sigma}\,\bar{a}. \tag{9}$$

The equation for combined tension and bending from [12] is:

$$\sigma_T + \frac{1+\nu}{3+\nu} \cdot \sigma_B = \frac{K}{\sqrt{\pi a}} \tag{10}$$

and hence we have:

$$\sigma_B = \frac{3+\nu}{1+\nu} \cdot \frac{K}{\sqrt{\pi a}} - \frac{3+\nu}{1+\nu} \frac{\bar{\sigma}\,\bar{a}}{a}. \tag{11}$$

For crack lengths less than $\bar{a}$ the distribution effect will not apply and the tensile stress will remain constant at $\bar{\sigma}$ giving:

$$\sigma_B = \frac{3+\nu}{1+\nu} \cdot \frac{K}{\sqrt{\pi a}} - \frac{3+\nu}{1+\nu} \cdot \bar{\sigma} \tag{12}$$

for $a < \bar{a}$.

At higher values of $1/\sqrt{a}$ the results tend to a line of the correct slope which from equation (12) gives a value of $\bar{\sigma} = 1{,}410$ lbf/in. The divergence from this line takes place at $1/\sqrt{a} = 4{\cdot}6$, i.e. $\bar{a} = 0{\cdot}0475$ ins and using this value in equation (11) gives the line shown in Fig. 4. This is a good fit to the experimental points and the straight line transition takes place at about the maximum point of the first section. Thus bending effects with the interference effect may be predicted using the form of equation given in (11).

The results for the plates under lateral pressure which failed in bending agree with the same line (Fig. 8) and confirm the result. The criterion of $\sigma/t > 1$ for tensile failure is a good approximation and agrees with the tension results. It is of interest that some of the bending failures are quite near the theoretical line $(3+\nu)/(1+\nu) \times$ tension indicating that in some cases the interference effect was not active.

The pressure tests on tubes with both axial and circumferential cracks gave quite good agreement with the theory using a K_{Ic} value of 1,650 lbf/in$^{3/2}$. The reason for the lack of slow crack growth is probably the higher stored energy of the loading system giving rise to a rapid acceleration of the crack once it has started moving resulting in the rapid fracture K_{Ic} value. Interference effects in bending in this predominantly tensile stress are not large.

Conclusions

Tests with bending stress systems may be accurately described by modifying the theoretical equation to take into account the interference effects on the compression side of the cracks. For PMMA the form of the relationship may be taken as:

$$\sigma_B = \frac{3+\nu}{1+\nu} \cdot \frac{K}{\sqrt{\pi a}} - \frac{3+\nu}{1+\nu} \cdot \frac{\bar{\sigma}\,\bar{a}}{a}$$

for $a > \bar{a}$

and

$$\sigma_B = \frac{3+\nu}{1+\nu} \cdot \frac{K}{\sqrt{\pi a}} - \frac{3+\nu}{1+\nu} \cdot \bar{\sigma}$$

when $a < \bar{a}$

when $\bar{\sigma} = 1{,}410$ lbf/in^2 and $\bar{a} = 0{\cdot}0475$ ins.

For plates subjected to lateral pressure bending failures of this form were observed for $\delta/t < 1$ and conformed to the same relationship. For tests with large bulging effects ($\delta/t > 1$) a normal tensile criterion was satisfactory. Cylinders with both axial and circumferential cracks confirmed the theoretical expectations.

Acknowledgements

The authors wish to thank Mr N. Naylor who designed the apparatus and I.C.I. Reterochemical and Polymer Laboratory for valuable help

References

1. BROWN, W. F. & SRAWLEY, J. E. 'Plane strain crack toughness testing of high strength metallic materials', *ASTM. STP.*, p. 410, 1966.
2. PARIS, P. C. & SIH, G. C. 'Stress analysis of cracks', 'Fracture toughness testing', *ASTM. STP.*, vol. 381, pp. 30-83, 1965.
3. WILLIAMS, J. G., RADON, J. C. & TURNER, C. E. 'Designing against fracture in brittle plastics', *Polymer Eng. Sci.*, Vol. 8 (2), pp. 130-141, April, 1968.
4. SIH, G. C., PARIS, P. C. & ERDOGAN, F. 'Crack-tip, stress-intensity factors for plane extension and plate bending problems', *Trans. ASME*, E29, (2), pp. 306-312, June, 1962.
5. ERDOGAN, F., TUNCEL, O. & PARIS, P. C. 'An experimental investigation of the crack-tip stress intensity factors in plates under cylindrical bending', *Trans. ASME* D84 (4), pp. 542-546, Dec., 1962.
6. TIMOSHENKO, S. P. & WOINOWSKY-KRIEGER, S. 'Theory of plates and shells', 2nd ed., McGraw-Hill, New York, 1959.
7. SECHLER, E. E. & WILLIAMS, M. L. 'The critical crack length in pressurised, monocoque cylinders', Final report on Contract NAW-6562, California Institute of Technology, Sept., 1959.

8. FOLIAS, E. S. 'A finite line in a pressurised spherical shell', *Int. Jour. Fracture Mech.* Vol. 1, 1, pp. 20-46, March, 1965.
9. FOLIAS, E. S. 'An axial crack in a pressurised cylindrical shell', *Int. Jour. Fracture Mech.*, Vol. 1, 2, pp. 104-113, June, 1965.
10. FOLIAS, E.S. 'A circumferential crack in a pressurised cylindrical shell', *Int. Jour. Fracture Mech.*, Vol. 3, 1, pp. 1-10, March, 1967.
11. DUFFY, A. R., EIBER, R. J., MAXEY, W. A. & McCLURE, G. M. 'Research on steels for high pressure pipelines', Paper presented at Fifth Int. Pipes and Pipeline Eng. Convention, London, June, 1968.
12. ANG, D. D. & WILLIAMS, M. L. 'Combined stresses in an orthotropic plate having a finite crack', *Trans ASME*. E28, vol. 4, pp. 372-378, Sept., 1961..

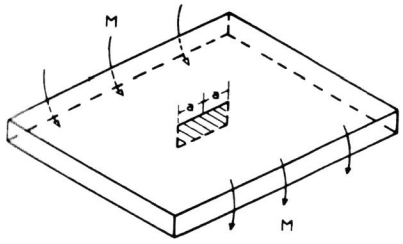

Fig. 1. Plate subjected to bending.

Fig. 2. Single edge notch tension results.

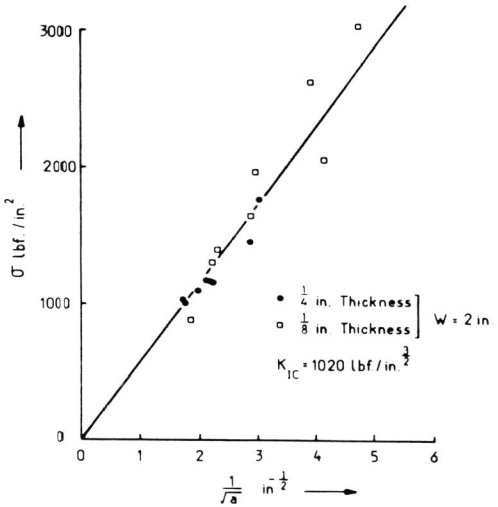

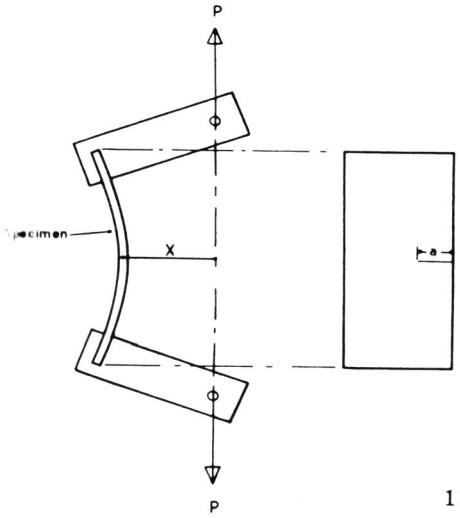

Fig. 3. Loading system for bending plates.

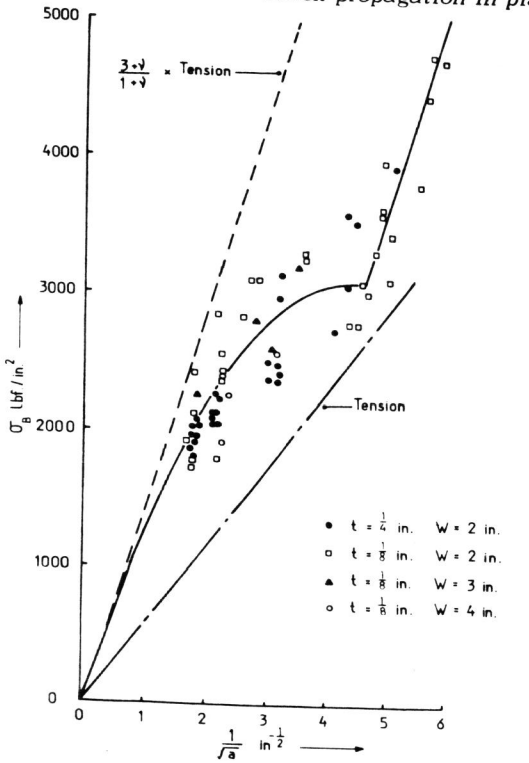

Fig. 4. Bending of plates.

Fig. 5. Elliptical slow crack growth in bending.

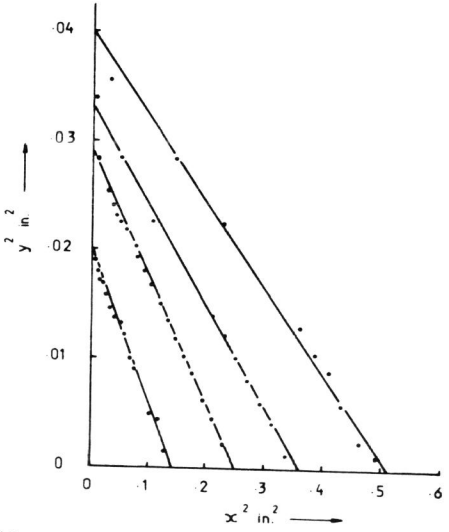

Fig. 6. Co-ordinates of slow growth areas.

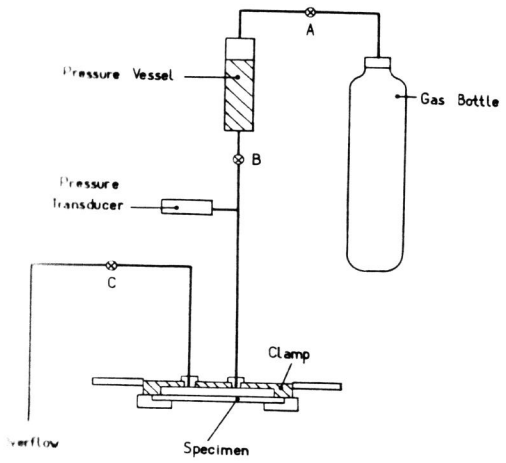

Fig. 7. Layout of pressure testing equipment.

Fig. 8. Plates subjected to lateral pressure.

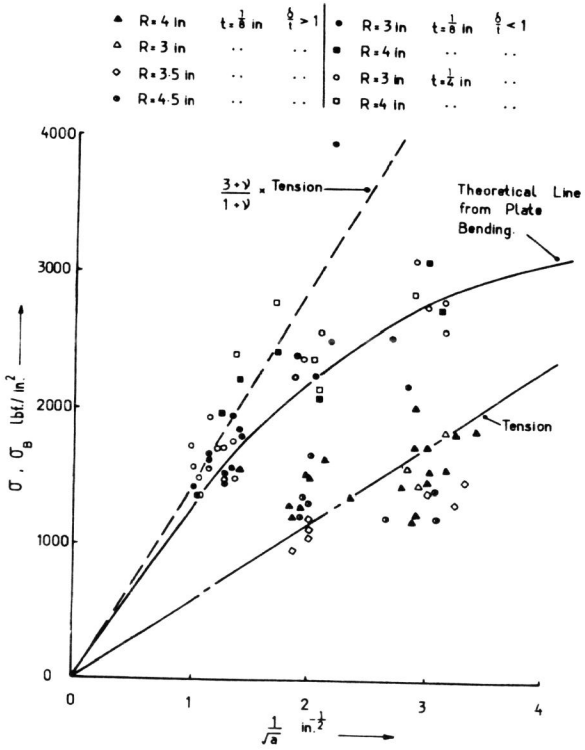

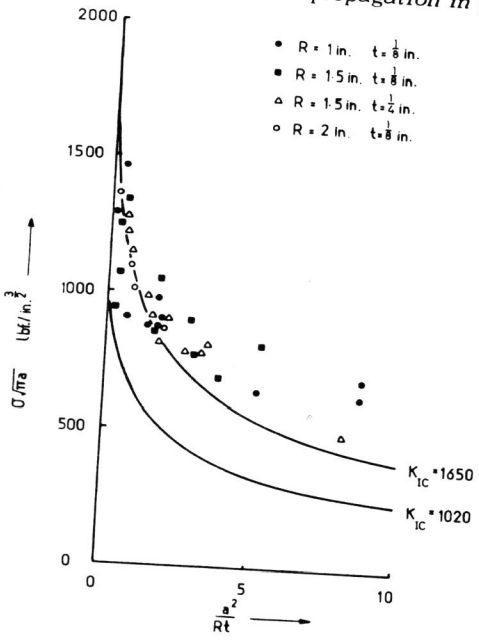

Fig. 9. Pressure tests on cylinders with axial cracks.

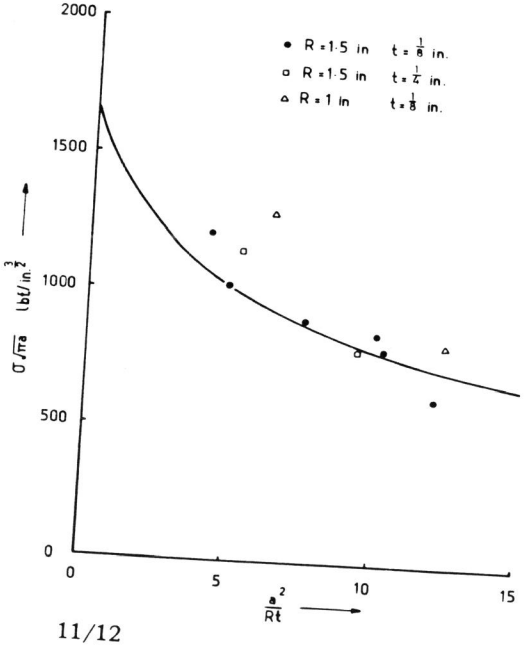

Fig. 10. Pressure tests on cylinders with circumferential cracks.